Chain-Length Dependence of the Structures and Phases of $CH_3(CH_2)_{n-1}SH$ Self-Assembled on Au(111)

P. Fenter[a] and P. Eisenberger

Department of Physics and Princeton Materials Institute, Princeton University, Princeton, New Jersey 08540

K. S. Liang

Exxon Corporate Research, Annandale, New Jersey 08801

(Received 19 October 1992)

A grazing incidence x-ray diffraction study of $CH_3(CH_2)_{n-1}SH$ self-assembled on a Au(111) surface shows that self-assembly results in a nonequilibrium state with a specific defect structure. We also explore the global (n,T) phase diagram whose phases are distinguished by the tilt direction and the two-dimensional periodicity. These phases result in distinct long ($n > 14$) and short ($n < 14$) chain-length regimes, and reflect the relative importance of the hydrocarbon and interface interactions in these systems.

PACS numbers: 68.35.Rh, 61.10.Lx, 61.66.Hq

Organic monolayers, which were first studied over 200 years ago [1], typically consist of a densely packed lattice of long-chain hydrocarbon molecules which are oriented largely perpendicular to the layer and interact laterally through van der Waals interactions. In spite of this simplicity, these systems [such as Langmuir [2] and Langmuir-Blodgett [3] (LB) monolayers] continue to be a fertile area of study with relevance to such diverse fields as two-dimensional melting, membranes, protective layers, biological sensors, and artificial molecular architectures [4]. Langmuir monolayers are known to exhibit numerous phase transitions and are under thermodynamic control [2], while LB monolayers and multilayers (which are weakly bound to solid substrates) are known to be largely metastable, exhibiting strongly irreversible thermal behavior at elevated temperatures [3].

Self-assembled monolayers (SAM) are a comparatively new type of organic monolayer [4,5] which form by the spontaneous *chemisorption* of functionalized long-chain molecules from solution to many different solid substrates (e.g., Au, Ag, Cu, Al, Si). The most thoroughly studied and best characterized SAM system is $CH_3(CH_2)_{n-1}SH(C_n)$ adsorbed on a Au(111) surface. This system has been previously studied by many experimental techniques such as IR spectroscopy, ellipsometry, and electron, He, and x-ray diffraction [6–8]. The consensus from these studies is that, in all cases, the monolayer adopts a simple commensurate $\sqrt{3}\times\sqrt{3}R30°$ overlayer structure. Yet while simple packing arguments and IR spectroscopy results suggest a $\sim(30\pm10)°$ tilt [7], x-ray diffraction measurements [8] find a 10° tilt. In addition, molecular dynamics simulations [9] have predicted the existence of "rotator" phases above 250 K, which would suggest a similarity of this system to the bulk n alkanes [10,11].

At present there exists only rudimentary knowledge of the properties of the C_n/Au(111) system at the molecular level. Consequently, we have undertaken a detailed study of the properties of this system using grazing incidence x-ray diffraction, covering a wide range of chain lengths, including $n = 10$, 12, 14, 16, 18, 22, 30. In this paper, we describe the main results of this study focusing on two major points. First of all, we discuss the two-dimensional structure of the monolayer, and show that the as-deposited state (when prepared under typical conditions) has only a limited domain size due to the self-assembly process, and in addition is characterized by a specific defect structure. Second, we map out the global (n,T) phase diagram. From measurements of both the tilt structure (i.e., the tilt angle and tilt direction) and striking differences in the high-temperature phase behavior, we find distinct long ($n > 14$) and short ($n \leq 12$) chain-length regimes. These phases reflect the relative importance of the "hydrocarbon" and "interface" interactions in these systems, resulting in a more complex structural phase diagram than previously believed.

We have taken care to prepare monolayers of the highest quality. To this end, we use Au(111) single crystal substrates prepared by standard UHV techniques, resulting in the expected $\sqrt{3}\times23$ surface reconstruction [12]. The monolayers are formed [6] by self-assembly in a dilute (~1 mM) solution of C_n in ethanol, and after completion ($\sim$24–48 h) are stored under a dry nitrogen atmosphere (typically less than 2 weeks). The measurements were performed at the Exxon X10A beamline at the National Synchrotron Light Source using the "Z-axis" surface spectrometer at a fixed incident angle of $\sim0.4°$ and an x-ray wavelength of 1.09 Å. The sample was kept under vacuum ($P \approx 10^{-8}$ Torr) during the measurements; we have found that under these conditions, these monolayers are very insensitive to beam damage [13], although some changes could be observed after extended exposure.

We first discuss the two-dimensional structure of the monolayer. A schematic of the C_n/Au(111) structure in both real and reciprocal space is shown in Figs. 1(a) and 1(b), respectively. In Fig. 1(c), we show radial scans

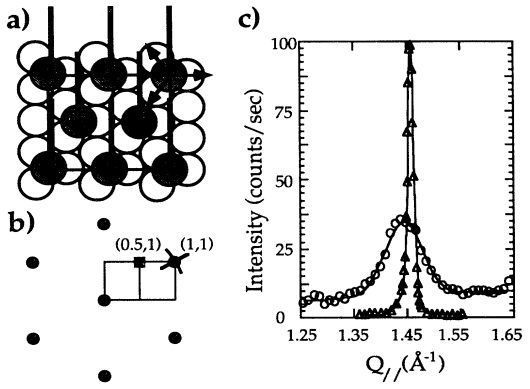

FIG. 1. (a) Top view of the surface indicating Au (open circles) and S atoms (shaded circles), a NNN tilt of the hydrocarbon chains (vertical solid lines), the superlattice unit cell, and the direction of a lateral displacement of top layer Au atoms (arrows). (b) 2D reciprocal space structure of the hexagonal $\sqrt{3}\times\sqrt{3}R30°$ lattice (circles) and one domain of the superlattice structure (square) showing the (0.5,1) peak. (c) Radial scan through the (1,1) diffraction peak of C_{12}, as deposited ($Q_z=0.40$ Å^{-1}, circles) and after an anneal ($Q_z=0.19$ Å^{-1}, triangles).

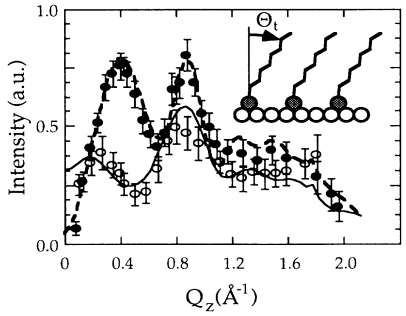

FIG. 2. Rod scan data and calculations of the (1,1) peak for both C_{12} (open circles) and C_{18} (closed circles). The data were taken with a resolution of $\Delta Q_{\|}=0.2$ Å^{-1} and $\Delta Q_z=0.04$ Å^{-1}. These calculations are full structure factor calculations, and the models are described in the text. The inset shows a side view of the surface, with Au and S atoms, and the tilted hydrocarbon chains.

through the (1,1) diffraction peak [indexed with a rectangular cell; see Fig. 1(b)] of a C_{12} monolayer, both "as deposited" and after an anneal to 90 °C. From the annealed peak position in the radial scan, $Q_{\|}=1.455\pm0.004$ Å^{-1}, as well as its azimuthal orientation ($\phi=30°$), we find that the monolayer forms the expected $\sqrt{3}\times\sqrt{3}R30°$ structure. We have also observed higher order diffraction peaks from this hexagonal structure, as well as many other peaks due to a superlattice [14] whose unit cell consists of a doubling of the traditional herringbone unit cell [11] along the short axis as indicated in Fig. 1(b). From the width of the as-deposited (1,1) peak ($\Delta Q_{\|}=0.07$ Å^{-1}), we find that the monolayer has a domain size of ~90 Å (which is characteristic of all the as-deposited SAMs that we have studied), while the annealed linewidth has a domain size of > 1000 Å (the annealed line shape is resolution limited) and is comparable to the substrate domain size. Consequently, defects play an important role in the as-deposited monolayer, and the limited order is due to a kinetic limitation in the self-assembly process.

We next address the nature of the defects in the as-deposited state. We note that there is a clear (~1%) *shift* of the as-deposited diffraction peak from the commensurate position which coincides with the narrow peak position in Fig. 1(c). This shift is part of a systematic *modulation* of the $\sqrt{3}$ structure, with the (2,2) peak exhibiting a shift of the same size but in the opposite direction. This behavior is characteristic of a system that is locally commensurate, but with domain walls which have a different spacing. For a $\sqrt{3}\times\sqrt{3}R30°$ overlayer, the phase difference between adjacent domains is $\pi/3$ and $2\pi/3$. From model calculations which assume a random distribution of domain walls [15], the fractional shift, $\delta=(Q_{22}-2Q_{11})/(Q_{22}+Q_{11})$, is proportional to the difference in the number of these two defects $N_{\pi/3}-N_{2\pi/3}$. From the peak shift in the as-deposited structure, $\delta=0.009$, we find that the $\pi/3$ defect is preferred, with a relative concentration of ~60%. Earlier measurements have found that the self-assembly process in this system is characterized by a rapid initial adsorption, followed by a slower completion of the monolayer [16]. Since the initial deposition (which may proceed through either nucleated island growth or random deposition) will result in equal numbers of these two defects, our results strongly suggest that the completion process involves a reorganization of the *defects*. In addition, since it is the smaller ($\pi/3$) defects which are more prevalent, it is reasonable to infer that the mechanism for the reorganization is the local rearrangement near the $2\pi/3$ defects to allow some additional adsorption.

We now concentrate on the effect of chain length upon the tilt structure of the monolayer. In Fig. 2, we show a rod scan (i.e., the intensity variation *perpendicular* to the surface) of the (1,1) diffraction peak as a function of Q_z for both C_{12} and C_{18}. The scattering intensity due to the monolayer (which is found by performing azimuthal scans at each Q_z and fitting each of these scans to a peak and a linear background) is then corrected for resolution and Lorentz factors. The peak positions in the rod scans can be directly related to the magnitude of the chain tilt θ_t and the tilt direction (with respect to $Q_{\|}$ vector) Ψ [8,17]:

$$Q_z=Q_{\|}\tan(\theta_t)\cos(\Psi)\,. \tag{1}$$

Because of the sixfold symmetry of the Au(111) surface, $\Psi=0°$, $\pm60°$, ($\pm120°$,$180°$) for a next-nearest-neighbor (NNN) tilt, and $\Psi=\pm30°$, $\pm90°$, ($\pm150°$) for a nearest-neighbor (NN) tilt, where the tilt directions

in parenthesis are unobservable in our scattering geometry. From this relation, the C_{18} data (with peaks at $Q_z = 0.4$ and 0.9 Å^{-1}) indicate a NNN tilt of $\sim 30°$.

Because the C_{18} monolayer is ~ 22 Å thick, the rod scan peaks in Fig. 2 should have widths of $\Delta Q_z \sim 2\pi/22$ Å~ 0.3 Å^{-1}. In addition to these peaks, both monolayers exhibit a significant and smoothly varying intensity at large Q_z, which we have observed at all chain lengths, and is due to the monolayer/substrate *interface*. That is, the top layer Au atoms are laterally relaxed away from their bulk lattice sites [see Fig. 1(a)], as is common in chemisorbed systems. Assuming a unique tilt direction, a structure factor analysis [18] of these data reveals that the C_{18} monolayer is tilted by $(30.3 \pm 0.5)°$ in a direction $(8.2 \pm 0.5)°$ from the NNN direction, with a lateral relaxation of Au atoms of 0.06 and -0.04 Å in the first and second layers, respectively.

This structure results in an interchain spacing (perpendicular to the chains) of 4.5 Å and resembles the local packing arrangement of the odd n alkanes [10,11], in which an equivalent ideal packing consists of a NNN tilt of 35° and a unit cell with dimensions of 4.96 Å×9.0 Å [19]. Consequently, in order to achieve commensurability with the $\sqrt{3}\times\sqrt{3}R30°$ lattice (which has a rectangular unit cell dimensions of 4.997 Å×8.655 Å), the hydrocarbon chains have undergone a 4% uniaxial compression in the NNN direction. This is most likely the source of both the off symmetry tilt direction and the superlattice structure that we have observed. We find that this structure is characteristic for $n = 16$, 18, 22, and 30, which implies that it satisfies both the *commensurability* and *hydrocarbon packing* constraints. As n decreases below 14, the tilt direction begins to shift further away from the symmetry direction resulting in a more highly *strained* chain packing configuration. In particular, for C_{12} we find a tilt angle of $(32.5 \pm 1)°$ in a direction $(13.8 \pm 2)°$ away from the NN direction, a nearly identical structure for C_{10}, and an intermediate tilt structure for C_{14}. This is the first indication that the short chain-length monolayers are dominated by the commensurability constraint, even at the expense of a strained hydrocarbon packing (i.e., it is *interface* dominated).

Finally, we discuss the dependence of the structure upon temperature. In Fig. 3, we show the evolution of the (1,1) peak as a function of temperature for annealed C_{12} and C_{14} monolayers. It is immediately apparent from these data that the C_{14} peak is broader than the C_{12} peak, and the evolution of the peak shape is very different in the two cases. The C_{12} monolayer does not exhibit any change in structure factor (including peak width or peak position) over the entire temperature range, having only a change in peak intensity. In contrast, the C_{14} monolayer undergoes a peak splitting which is direct evidence of a 2D structural phase transition above 60 °C to a nonhexagonal structure which is *incommensurate* with the substrate Au surface. In both cases, at a sufficiently high temperature the scattering intensity goes to zero, and upon cooling the structure reverts to the room-temperature hexagonal structure. Since these observations are characteristic of the thermal behavior of the $n \leq 12$ and $n \geq 14$ regimes, they further support the contention that these monolayers exhibit distinct "short" and "long" chain-length behavior.

In order to understand the nature of this disordering, we plot in Fig. 4 the peak intensity of both the (1,1) and (2,2) peaks for the C_{12} monolayer as a function of temperature. At $T = 50$ °C, a distinct change in slope occurs for both the (1,1) and (2,2) peaks which indicates the presence of a phase transition at this temperature. We have found that both the 2D structure (including both the hexagonal and superlattice structures; see Fig. 1) as well as the rod structure are preserved through this transition. In particular, the presence of the superlattice above 50 °C rules out the "rotator" phases [10,11] which had been predicted for this system [9].

We conclude that the transition in Fig. 4 is a simple melting transition; that is, a liquidlike phase of C_{12} exists on the surface above 50 °C. We can rule out an anomalous Debye-Waller effect since the rate at which the intensity decreases (above 50 °C) is the same for both the

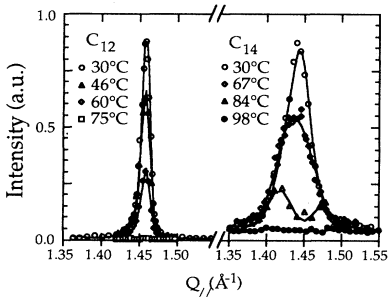

FIG. 3. Temperature-dependent structure factor as measured by a radial scan through the (1,1) peak for annealed samples of C_{12} and C_{14}. Note that although the structure factor of C_{12} does not change with temperature, the C_{14} structure factor splits above 60 °C.

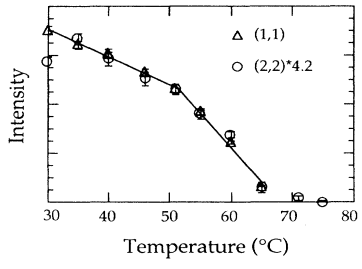

FIG. 4. The variation of the (1,1) and (2,2) peak intensity (at $Q_z = 0.19$ Å^{-1}) as a function of temperature for C_{12}. These data show a clear break at 50 °C, indicating a melting transition.

(1,1) and (2,2) peaks, and because the hydrocarbon and interface components (see Fig. 2) of the structure factor (which have very different vibrational amplitudes) *both* decrease in this transition. In the range 50–70 °C we believe that there is coexistence between the solid and liquid phases. Upon cooling the monolayer intensity returns to within $<4\%$ of its original value, and consequently desorption is minimal in this temperature range. We have not observed, and do not expect to observe, any scattering from a liquid monolayer because simple estimates predict that the peak intensity from this phase will be much weaker.

The complex phase behavior of the long-chain monolayers helps to explain why the annealed C_{14} sample in Fig. 3 has only a limited ($\sim$200 Å) coherence length in the hexagonal phase: We have found that the commensurate-incommensurate transition in the long-chain monolayers is hysteretic, and that it is possible to become "trapped" in the incommensurate phase at room temperature. We suspect that this is due, in part, to the slower kinetics of these long-chain molecules; further support for this conjecture is the observation that the C_{14} domain size increased from 90 Å (as deposited) to 400 Å in the incommensurate phase and then *decreased* to 200 Å upon cooling to the hexagonal phase. Except for these dramatic changes in peak width and splitting, we have found no evidence for a change in the *line shape* through these transitions.

These results provide a comprehensive picture of the C_n/Au(111) system which shows that the as-deposited monolayers are characterized by a limited coherence length as well as a modulation caused by an incomplete reorganization in the self-assembly process. At all chain lengths, we find a strained structure with both a low symmetry tilt and a superlattice structure, which melts at temperatures that are $\sim$60 °C above the melting temperatures of the bulk *n* alkanes. This shows that the SAM's properties deviate from typical *n*-alkane behavior because of the chemisorption to the surface. From both the tilt structure and the thermal behavior, we find distinctive properties for "long" and "short" chain lengths, resulting in a phase diagram which is much richer than previously believed. Since the relative strength of the hydrocarbon and interface interactions is controlled by varying the chain length, these results should be general to all SAM systems, although the detailed phase behavior will depend greatly upon the strength of the monolayer/substrate interaction and the degree of strain present in the commensurate structure.

We would like to acknowledge the close interaction with J. Li, N. Camillone III, Dr. G.-Y. Liu, and Dr. T. A. Ramanarayanan throughout these studies, and especially Dr. G. Scoles for his insight and support. In addition, P.F. would like to thank H. H. Hung for help at the initial phase of these studies, and Dr. L. D. Gibbs and Dr. E. B. Sirota for helpful discussions. This work was performed at the NSLS which is supported by DOE Contract No. DE-AC0276CH-00016.

[a]Also at Exxon Corporate Research, Annandale, NJ 08801.

[1] B. Franklin, Philos. Trans. R. Soc. London **64**, 444 (1774).

[2] M. C. Shih, T. M. Bohanon, J. M. Mikrut, P. Zschack, and P. Dutta, Phys. Rev. A **45**, 5734 (1992); R. M. Kenn, C. Bohm, A. M. Bibo, I. R. Paterson, H. Mohwald, J. Als-Neilsen, and K. Kjaer, J. Phys. Chem. **95**, 2092 (1991).

[3] P. Tippman-Krayer, H. Mohwald, and Yu. M. L'vov, Langmuir **7**, 2298 (1991); A. Ulman, Adv. Mater. **3**, 298 (1991).

[4] J. D. Swalen, D. L. Allara, J. D. Andrade, E. A. Chandross, S. Garoff, J. Israelachvili, T. J. McCarthy, R. Murray, R. F. Pease, J. F. Rabolt, K. J. Wynne, and H. Yu, Langmuir **3**, 932 (1987).

[5] L. H. Dubois, and R. G. Nuzzo, Annu. Rev. Phys. Chem. **43**, 437 (1992).

[6] L. Strong and G. M. Whitesides, Langmuir **4**, 546 (1988).

[7] R. G. Nuzzo, L. H. Dubois, and D. L. Allara, J. Am. Chem. Soc. **112**, 558 (1990).

[8] M. G. Samant, C. A. Brown, and J. G. Gordon II, Langmuir **7**, 437 (1991).

[9] J. Hauptman and M. L. Klein, J. Chem. Phys. **93**, 7483 (1990).

[10] J. Doucet, I. Denicolo, and A. Craievich, J. Chem. Phys. **75**, 1523 (1981).

[11] E. B. Sirota, H. E. King, Jr., D. M. Singer, and H. Shao (to be published).

[12] A. R. Randy, S. G. J. Mochrie, D. M. Zehner, K. G. Huang, and D. Gibbs, Phys. Rev. B **43**, 4667 (1991).

[13] P. Fenter, J. Li, P. Eisenberger, T. A. Ramanarayanan, and K. S. Liang, in *Interface Dynamics and Growth*, edited by K. S. Liang *et al.*, MRS Symposia Proceedings No. 237 (Materials Research Society, Pittsburgh, 1992), p. 291.

[14] N. Camillone III, C. E. D. Chidsey, G.-Y. Liu, and G. Scoles (to be published).

[15] P. Fenter and T.-M. Lu, Surf. Sci. **154**, 15 (1985).

[16] C. D. Bain, E. B. Troughton, Y.-T. Tao, J. Evall, G. M. Whitesides, and R. G. Nuzzo, J. Am. Chem. Soc. **111**, 321 (1989).

[17] G. S. Smith, E. B. Sirota, C. R. Safinya, R. J. Plano, and N. A. Clark, J. Chem. Phys. **92**, 4519 (1990).

[18] P. Fenter, P. Eisenberger, and K. S. Liang (unpublished).

[19] A. I. Kitaigorodskii, *Organic Chemistry Crystallography* (Consultants Bureau, New York, 1961).